

AG  
T

*Algebraic & Geometric  
Topology*

Volume 23 (2023)

**Unchaining surgery, branched covers,  
and pencils on elliptic surfaces**

TERRY FULLER



# Unchaining surgery, branched covers, and pencils on elliptic surfaces

TERRY FULLER

R İnanç Baykur, Kenta Hayano, and Naoyuki Monden used a technique called *unchaining* to construct a family of simply connected symplectic 4–manifolds  $X'_g(i)$  for all  $g \geq 3$  and  $0 \leq i \leq g - 1$  (*Geom. Topol.* 20 (2016) 2335–2395). Among this family, the manifolds  $X'_g(g - 2)$  are shown to be symplectic Calabi–Yau 4–manifolds. They also showed that each  $X'_g(i) \# \overline{\mathbb{C}\mathbb{P}^2}$  admits a pair of inequivalent genus  $g$  Lefschetz pencils. We show how to describe every  $X'_g(i)$  as a 2–fold branched cover of a rational surface, and use this to prove that each  $X'_g(i)$  is diffeomorphic to the elliptic surface  $E(g - i)$ . This has several notable consequences: each symplectic Calabi–Yau they construct is diffeomorphic to K3; for each  $n \geq 3$  and  $g \geq n$ , the elliptic surface  $E(n)$  admits a genus  $g$  Lefschetz pencil; and for each  $n \geq 3$  and  $g \geq n$ , the once blown up elliptic surface  $E(n) \# \overline{\mathbb{C}\mathbb{P}^2}$  admits a pair of inequivalent genus  $g$  Lefschetz pencils.

57K40, 57K43

## 1 Introduction

Since the foundational work of Donaldson [6] and Gompf [10] in the 1990s, Lefschetz pencils and fibrations have been known to characterize symplectic 4–manifolds. In [4], R İnanç Baykur, Kenta Hayano, and Naoyuki Monden construct a doubly indexed family of symplectic 4–manifolds  $X'_g(i)$  for all  $g \geq 3$  and  $0 \leq i \leq g - 1$ . Their examples are constructed as the total spaces of symplectic genus  $g$  Lefschetz pencils, through explicit factorizations of their monodromy. We review the specific factorizations which define  $X'_g(i)$  below, but in the meantime summarize results from [4] about these manifolds:

**Theorems** [4] *For each  $g \geq 3$  and  $0 \leq i \leq g - 1$ , there is a genus  $g$  Lefschetz pencil on  $X'_g(i)$  with the following properties:*

- (a) [4, Lemma 4.7] The manifolds  $X'_g(i)$  are simply connected, with Euler characteristic  $e(X'_g(i)) = 12(g - i)$  and signature  $\sigma(X'_g(i)) = -8(g - i)$ .
- (b) [4, Lemma 5.6] The manifolds  $X'_g(i)$  are spin if and only if  $g - i$  is even.
- (c) [4, Theorem 4.8] The manifolds  $X'_g(g - 1)$  are diffeomorphic to the rational elliptic surface  $E(1)$ .

These statements suggest our main result:

**Theorem 1** The manifolds  $X'_g(i)$  are diffeomorphic to the elliptic surface  $E(g - i)$ .

This has some immediate corollaries. In [4], Baykur, Hayano, and Monden note that when  $g - i$  is even,  $X'_g(i)$  is irreducible (since it is spin), but the irreducibility of  $X'_g(i)$  for odd  $g - i$  is left open.

**Corollary 2**  $X'_g(i)$  is irreducible for all  $g \geq 3$  and  $0 \leq i \leq g - 2$ .

Additionally, in [4], the Kodaira dimensions of  $X'_g(i)$  are computed only for the special cases of  $g - 3 \leq i \leq g - 1$  and  $g - i$  even. Our main theorem fills in the missing cases:

**Corollary 3** The symplectic Kodaira dimension of  $X'_g(i)$  is

$$(1) \quad \kappa(X'_g(i)) = \begin{cases} -\infty & \text{if } i = g - 1, \\ 0 & \text{if } i = g - 2, \\ 1 & \text{if } 0 \leq i \leq g - 3. \end{cases}$$

An additional corollary concerns *symplectic Calabi–Yau 4–manifolds*. A complex Calabi–Yau surface is one with a trivial canonical class, and one can likewise define a symplectic Calabi–Yau 4–manifold to be one with a trivial symplectic canonical class. All known examples of symplectic Calabi–Yau manifolds are complex K3 surfaces or torus bundles over tori. Since any symplectic Calabi–Yau manifold must have the rational homology type of these complex surfaces (see Bauer [2] and Li [13]), it is an intriguing open question if there exist *any* symplectic Calabi–Yau 4–manifolds which are not diffeomorphic to one of these; see Friedl and Vidussi [8] and Li [14]. Baykur, Hayano, and Monden show that the manifolds  $X'_g(g - 2)$  are symplectic Calabi–Yau [4, Corollary 4.10], and ask if they are diffeomorphic to the standard K3 surface.

**Corollary 4** The symplectic Calabi–Yau manifolds  $X'_g(g - 2)$  are diffeomorphic to K3.

In addition to its relevance to finding examples of symplectic Calabi–Yau manifolds, this result serves to illustrate the diversity of Lefschetz pencils on fixed 4–manifolds. The K3 surface is known to admit pencils of every genus (see Smith [15]), and it is noted in [4] that the diffeomorphism  $X'_g(g-1) \cong E(1)$  implies that the same is true for the rational elliptic surface  $E(1)$ . The author is not aware of any other such examples.

**Corollary 5** *For all  $n \geq 3$ , the elliptic surface  $E(n)$  admits a genus  $g$  Lefschetz pencil for every  $g \geq n$ .*

A deeper related application concerns finding inequivalent Lefschetz pencils on a given 4–manifold with the same topological data (ie genus and number of basepoints). By using the braiding lantern substitution technique of Baykur and Hayano [3], Baykur, Hayano, and Monden prove:

**Theorem** [4, Corollary 6.4] *For all  $g \geq 3$  and  $0 \leq i \leq g-1$ , the manifold  $X'_g(i) \# \overline{\mathbb{C}\mathbb{P}^2}$  admits a pair of inequivalent genus  $g$  Lefschetz pencils. In particular, the manifold  $E(1) \# \overline{\mathbb{C}\mathbb{P}^2}$  admits a pair of inequivalent genus  $g$  Lefschetz pencils for all  $g \geq 3$ .*

[Theorem 1](#) strengthens this result.

**Corollary 6** *For all  $n \geq 3$ , the once blown up elliptic surface  $E(n) \# \overline{\mathbb{C}\mathbb{P}^2}$  admits a pair of inequivalent genus  $g$  Lefschetz pencils for all  $g \geq n$ .*

Of course, the conclusions of corollaries 5 and 6 apply to blow ups of  $E(n)$  and  $E(n) \# \overline{\mathbb{C}\mathbb{P}^2}$  at basepoints, as well.

The method of proof of [Theorem 1](#) exploits the natural 2–fold symmetry of Baykur, Hayano, and Monden’s construction. We begin by blowing up the pencil on  $X'_g(i)$  to obtain an associated Lefschetz fibration  $X_g(i)$ , and use this symmetry to represent  $X_g(i)$  as a 2–fold branched cover of a rational surface. A sequence of handle slides in the base of this cover allows one to find and blow down the required number of exceptional sections, and we arrive at a branched cover description of  $X'_g(i)$ . The branch surface of this cover is represented as a banded unlink diagram, of the sort studied by Mark Hughes, Seungwon Kim, and Maggie Miller in [11], with an explicitly drawn ribbon surface as (most of) the branch locus. We then use various band moves to obtain an isotopy of the branch surface, yielding a branched cover description that is recognized as one for elliptic surfaces.

In [Section 2](#) we discuss banded unlink diagram descriptions of embedded surfaces, and review the moves on these diagrams that we will employ in the proof. The following section reviews the topology of Lefschetz pencils and fibrations. Finally, in [Section 4](#), we define the manifolds  $X'_g(i)$  and  $X_g(i)$ , and give the proof of [Theorem 1](#).

## 2 Banded unlink diagrams

In this section we review the notion of a banded unlink diagram [\[11\]](#). This describes a closed surface embedded in a closed 4-manifold  $X$ . Banded unlink diagrams can be defined using any handlebody description for  $X$ , but since in our application  $X$  will lack 1- and 3-handles, we only discuss that setting here.

Suppose  $X$  is obtained by attaching  $n$  2-handles to a single 0-handle, and then attaching one 4-handle. The manifold  $X$  can be depicted by a Kirby diagram  $\mathcal{K}$  consisting of an  $n$ -component framed link in  $S^3$ . Let  $X_0$  denote the boundary of the 0-handle, and  $X_1$  the union of the 0- and 2-handles. Of course, both  $\partial(X_0)$  and  $\partial(X_1)$  are  $S^3$ , and  $\partial(X_1)$  can be described as the result of a surgery of  $S^3$  along the components of  $\mathcal{K}$ .

Let  $L$  be a link in the exterior  $E(\mathcal{K})$ . Since  $L$  avoids the attaching region of the 2-handles, we can view  $L$  as a link in  $\partial(X_0)$  and in  $\partial(X_1)$ . In a banded unlink diagram, we begin with an unlink in  $E(\mathcal{K})$ , and form a ribbon surface by attaching a disjoint collection of bands to the spanning disks of the unlink;  $L$  is the link that results from the band surgery to the unlink, and we may push the interior of the ribbon surface into  $X_0$  to get an embedded surface. In a banded unlink diagram, we also require that  $L$  bounds a collection of disjoint disks in  $\partial(X_1)$ . In this way, the ribbon surface that  $L$  bounds can be capped off by these disks, giving a closed surface in  $X$ .

In [\[11\]](#), Hughes, Kim, and Miller give a complete set of moves for banded unlink diagrams of isotopic surfaces in a 4-manifold. As we will apply these to manifolds without 1-handles, we review only the moves that we use later: band slides, band swims, 2-handle band swims, and 2-handle band slides. These are shown in [Figure 1](#). (The 2-handle band slides in [Figure 1](#) can be done with any knotted attaching circle and any framing, following the usual rules of Kirby calculus; the 0-framed unknot pictured here is all that will be used later. The strands running through the attaching circle of the handle can represent other handles, bands, or unlink components.)

Two particular iterations of the swim moves will be used often, and are shown in [Figures 2](#) and [3](#). In each figure, a sequence of swims is performed, moving the band

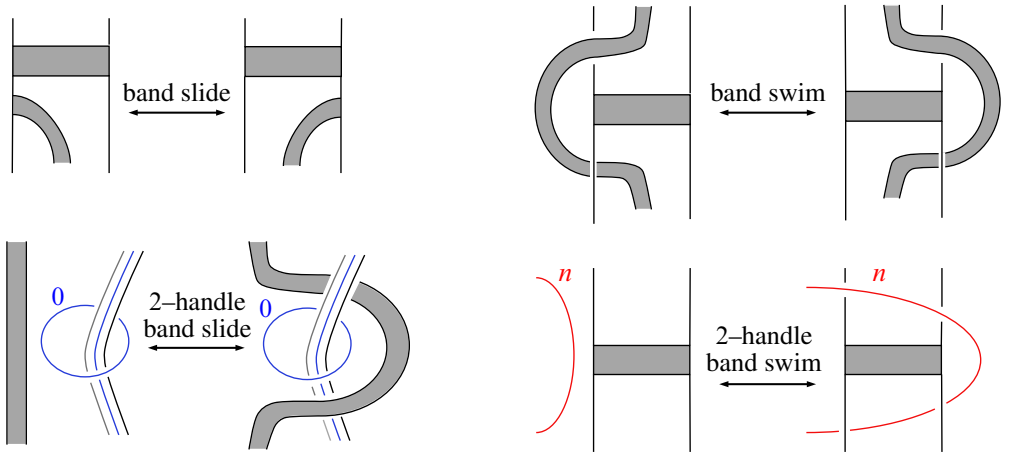


Figure 1: In the two swim moves, the band/attaching circle passes lengthwise through the interior of the horizontally drawn band.

or attaching circle from the right side of the initial diagram successively through each of the bands to its left. An intermediate step following the first swim is depicted in each figure. In later use, the initial ribbon surface from each figure will be replaced by

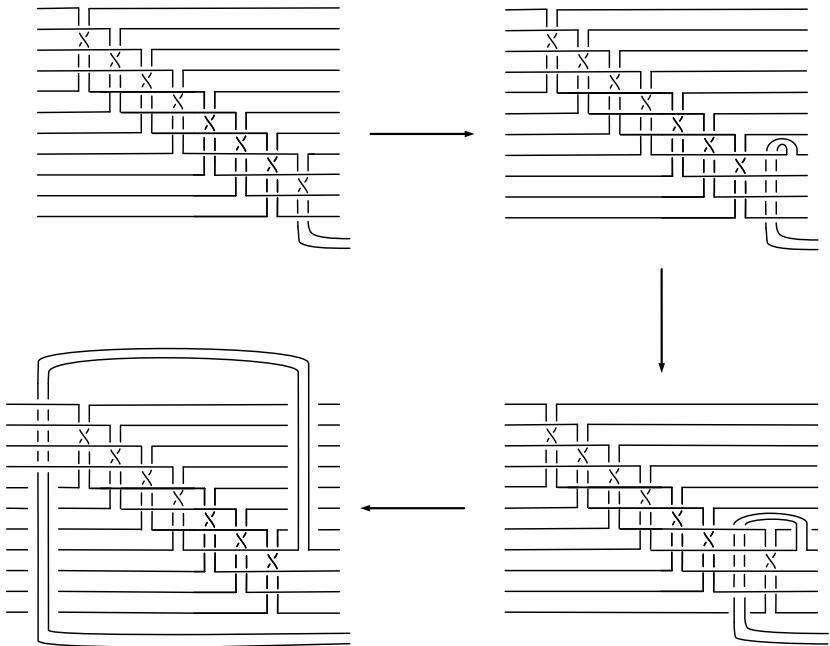


Figure 2: A band dive.

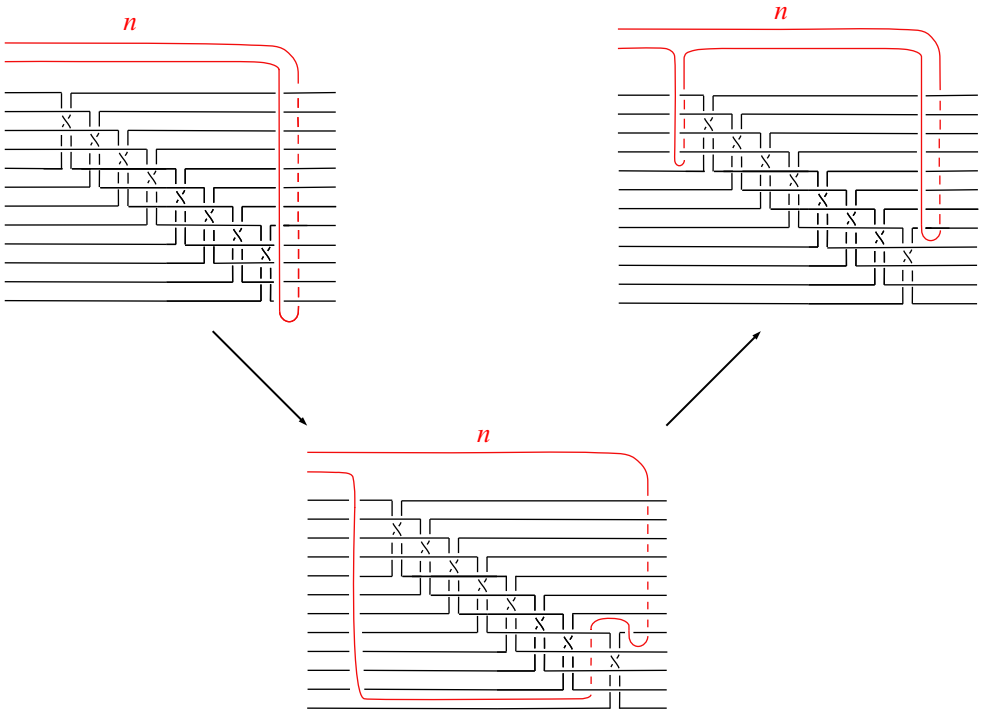


Figure 3: A 2-handle band dive.

the final one, and we will refer to these moves as *band dives* and *2-handle band dives*, respectively.

### 3 Lefschetz pencils and fibrations

In this section we review the definitions of Lefschetz fibrations and Lefschetz pencils, and discuss the topology of these structures. A more comprehensive description of the topology of Lefschetz fibrations and pencils can be found in [10].

We denote a closed oriented genus  $g$  surface by  $\Sigma_g$ , and a compact oriented genus  $g$  surface with  $n$  boundary components by  $\Sigma_g^n$ . Their mapping class groups will be denoted by  $\Gamma_g$  and  $\Gamma_g^n$ , respectively. We will also denote a sphere with  $m$  marked points by  $\Sigma_{0,m}$ , and its mapping class group by  $\Gamma_{0,m}$ .

**Definition** Let  $W$  be a compact oriented smooth 4-manifold, and  $C$  a compact oriented smooth surface. A proper smooth map  $f : W \rightarrow C$  is a *Lefschetz fibration* if

- (i) the critical points of  $f$  lie in the interior of  $W$ , and
- (ii) for each critical point of  $f$  in  $W$ , there are complex coordinate charts agreeing with the orientations on  $W$  and  $C$  such that locally  $f$  can be expressed as  $f(z_1, z_2) = z_1^2 + z_2^2$ .

We will only encounter  $C = S^2$  or  $D^2$ .

**Definition** Let  $W'$  be a closed oriented smooth 4–manifold. Let  $B \subset W'$  be a finite set of points. A smooth map  $f: W' \setminus B \rightarrow \mathbb{C}\mathbb{P}^1$  is a *Lefschetz pencil* if:

- (i) For each critical point of  $f$  in  $W' \setminus B$  there are complex coordinate charts agreeing with the orientations on  $W'$  and  $\mathbb{C}\mathbb{P}^1$  such that locally  $f$  can be expressed as  $f(z_1, z_2) = z_1^2 + z_2^2$ .
- (ii) For each point of  $B$  there is a complex coordinate chart on  $W'$  and an identification of the base as  $\mathbb{C}\mathbb{P}^1$  such that locally  $f$  can be expressed as  $f(z_1, z_2) = [z_1 : z_2]$ .

The existence of a Lefschetz pencil  $f: W' \setminus B \rightarrow \mathbb{C}\mathbb{P}^1$  will be described by saying that there is a Lefschetz pencil on  $W'$ .

The points of  $B$  are called *basepoints* of the Lefschetz pencil. A Lefschetz pencil with  $B = \emptyset$  is a Lefschetz fibration over  $\mathbb{C}\mathbb{P}^1 \cong S^2$ . If  $B \neq \emptyset$ , we can blow up  $W'$  at each basepoint to get  $W$ , and the Lefschetz pencil on  $W'$  becomes a Lefschetz fibration  $W \rightarrow \mathbb{C}\mathbb{P}^1 \cong S^2$ .

It is a consequence of these definitions that, for a Lefschetz fibration, a regular fiber  $f^{-1}(x)$  is a closed genus  $g$  surface. For a Lefschetz pencil with  $n > 0$  basepoints,  $f^{-1}(x)$  is not compact, and we instead consider  $f^{-1}(x) \cap (W' \setminus (U_1 \cup \dots \cup U_n))$ , where  $U_i$  is an open ball about the basepoint in each coordinate chart with property (ii) above. This fiber will be a compact genus  $g$  surface with  $n$  boundary components. We refer to *genus  $g$  Lefschetz fibrations or pencils*, accordingly.

Lefschetz pencils and fibrations are understood topologically through monodromy factorizations. Let  $x_1, \dots, x_\mu$  be the critical values for  $f$ . We assume, without loss of generality, that each critical point of  $f$  lies in a separate fiber. For a pencil, we select a regular value  $x_0 \in \mathbb{C}\mathbb{P}^1$ , and a disjoint collection of arcs  $\gamma_i$  from  $x_0$  to  $x_i$  for each  $i = 1, \dots, \mu$ . (We also assume each  $\gamma_i$  avoids the other critical points.) We further assume the arcs  $\gamma_1, \dots, \gamma_\mu$  appear in this order as we travel in a small circle about  $x_0$ . For each  $i$ , we consider a loop that begins at  $x_0$ , travels along  $\gamma_i$ , then counterclockwise around a small circle centered at  $x_i$ , and back to  $x_0$  along  $\gamma_i$ . Using



an identification of  $f^{-1}(x_0)$  with  $\Sigma_g^n$ , the monodromy of  $f$  along this loop is known to be a right-handed Dehn twist  $t_{c_i}$  along a simple closed curve  $c_i \subset \Sigma_g^n$  [12]. The curve  $c_i$  is called a *vanishing cycle*. To get a global description of a Lefschetz pencil, these local models must fit together according to the equation  $t_{c_1} \dots t_{c_\mu} = t_{\delta_1} \dots t_{\delta_n}$  in  $\Gamma_g^n$ , where  $\delta_j$  denotes a right-handed Dehn twist about a curve parallel to the  $j^{\text{th}}$  boundary component of  $\Sigma_g^n$ . Conversely, given any factorization in  $\Gamma_g^n$  of  $t_{\delta_1} \dots t_{\delta_n}$  as a product of right-handed Dehn twists, one can construct a Lefschetz pencil with monodromy prescribed by the factorization.

When working with Lefschetz fibrations, one has a similar description of the local monodromy about a critical value  $x_i$  as a right-handed Dehn twist  $t_{c_i}$  about a simple closed curve  $c_i \subset \Sigma_g$ . To form a global Lefschetz fibration over  $S^2$ , the local monodromies must concatenate to form a relation  $t_{c_1} \dots t_{c_\mu} = 1$  in  $\Gamma_g$ .

Any particular monodromy description of a Lefschetz pencil is far from unique, as it depends on a choice of identification of a regular fiber, as well as on a system of arcs  $\gamma_i$ . Modifying these choices translates into a simple set of moves on factorizations in  $\Gamma_g^n$  (see [10]), and two factorizations related in this way are said to be *Hurwitz equivalent*.

There is a straightforward relationship between a monodromy factorization of a Lefschetz pencil on  $W'$  and that of the Lefschetz fibration  $W \rightarrow S^2$  obtained by blowing up  $W'$  at all basepoints. Under the homomorphism  $\Gamma_g^n \rightarrow \Gamma_g$  obtained by capping off each boundary component of  $\Sigma_g^n$  with a disk, Dehn twists about the boundary parallel curves  $\delta_j$  become trivial in  $\Gamma_g$ . A monodromy factorization  $t_{c_1} \dots t_{c_\mu} = t_{\delta_1} \dots t_{\delta_n}$  in  $\Gamma_g^n$  for the pencil on  $W'$  then gives a monodromy factorization  $t_{c_1} \dots t_{c_\mu} = 1$  in  $\Gamma_g$  for the fibration  $W \rightarrow S^2$ .

A monodromy factorization of a genus  $g$  Lefschetz fibration  $f: W \rightarrow S^2$  also leads to a handlebody description of  $W$  in a well-understood way [10]. One begins with a handlebody description of  $\Sigma_g \times D^2$  consisting of a 0-handle, 1-handles, and 2-handles. Given a factorization  $t_{c_1} \dots t_{c_\mu} = 1$  in  $\Gamma_g$ , we form  $\Sigma_g \times D^2 \cup (\bigcup_{i=1}^\mu H_i^2)$ , where each  $H_i^2$  is a 2-handle attached along the vanishing cycle  $c_i$  in a separate fiber  $\Sigma_g \times \{\text{point}\} \subset \Sigma_g \times S^1 = \Sigma_g \times \partial D^2$ . The 2-handles are attached along the  $S^1$  factor in the order they appear in the factorization, and they have framing  $-1$  relative to the framing on  $c_i$  induced by the product  $\Sigma_g \times S^1$ . Following these handle attachments, we have a handlebody describing a Lefschetz fibration over  $D^2$  with the prescribed monodromy factorization. The boundary of  $\Sigma_g \times D^2 \cup (\bigcup_{i=1}^\mu H_i^2)$  is  $\Sigma_g$ -bundle over  $S^1$  with monodromy  $t_{c_1} \dots t_{c_\mu}$ ; because this is isotopic to the identity,

this boundary is diffeomorphic to  $\Sigma_g \times S^1$ . Hence we can extend the Lefschetz fibration to be one over  $S^2$  by attaching the trivial fibration  $\Sigma_g \times D^2 \rightarrow D^2$  along  $\Sigma_g \times S^1$ . This final attachment adds one or more 2–handles, 3–handles, and a 4–handle.

A technique for constructing new Lefschetz pencils or fibrations from old is *monodromy substitution*. Given a monodromy factorization, a monodromy substitution swaps a subword of the factorization with a different (but equal, in  $\Gamma_g^n$  or  $\Gamma_g$ ) product of right-handed Dehn twists. In [4], Baykur, Hayano, and Monden employ this operation using the *odd chain relation*: suppose  $c_1, c_2, \dots, c_{2h+1}$  are simple closed curves on  $\Sigma_g^n$  or  $\Sigma_g$  that form a chain; that is,  $c_i$  and  $c_{i+1}$  intersect in one point for all  $i$ , and  $c_i$  and  $c_j$  are disjoint otherwise. A regular neighborhood of  $c_1 \cup \dots \cup c_{2h+1}$  is a subsurface  $S$  homeomorphic to  $\Sigma_h^2$ . The chain relation is  $(t_{c_1} t_{c_2} \dots t_{c_{2h+1}})^{2h+2} = t_{b_1} t_{b_2}$ , where  $b_1$  and  $b_2$  are the boundary components of  $S$ . Using this relation to replace a subword in a monodromy factorization given by the left-hand side of the chain relation with the two Dehn twists on the right is referred to as *unchaining*.

**Realizing hyperelliptic Lefschetz fibrations as branched covers** Let  $\iota: \Sigma_g \rightarrow \Sigma_g$  be the hyperelliptic involution, and  $\pi: \Sigma_g \rightarrow \Sigma_{0,2g+2}$  the branched covering that is the quotient of  $\iota$ . A Lefschetz fibration on  $W \rightarrow S^2$  is *hyperelliptic* if it is Hurwitz equivalent to one with a monodromy factorization where each vanishing cycle  $c_i$  satisfies  $\iota(c_i) = c_i$ . If all  $c_i$  are nonseparating, then  $W$  is a 2–fold branched cover of an  $S^2$ –bundle over  $S^2$ , with the Lefschetz fibration map obtained as the composition of this cover with the bundle projection [9]. This cover is crucial to the proof of [Theorem 1](#), and we review the details.

Since all  $c_i$  are nonseparating and symmetric, the factorization  $t_{c_1} \dots t_{c_\mu} = 1$  is the lift of the relation  $h_{\pi(c_1)} \dots h_{\pi(c_\mu)} = 1$  in  $\Gamma_{0,2g+2}$ , where  $h_{\pi(c_i)}$  is a right-handed disk twist about the arc  $\pi(c_i)$  in  $\Sigma_{0,2g+2}$ . The factorization  $h_{\pi(c_1)} \dots h_{\pi(c_\mu)}$  can be used to construct a ribbon surface in  $S^2 \times D^2$ , for which the cover branched over that surface is a Lefschetz fibration over  $D^2$  with the required monodromy factorization. The Birman–Hilden theorem (see [5; 7]) then implies that we can always extend this cover by attaching a trivial covering of  $\Sigma_g \times D^2$  over  $S^2 \times D^2$ , resulting in  $W$  covering an  $S^2$ –bundle over  $S^2$  branched over a closed surface.

In practice, the base and branch set of this cover can be explicitly drawn as a banded unlink diagram. In  $S^2 \times D^2$ , represented as a Kirby diagram by a 0–framed unknot, we begin with  $2g + 2$  disks representing  $\{\text{point}\} \times D^2$ , drawn as meridians to the unknot, with their interiors pushed into the 0–handle. The branched cover of  $S^2 \times D^2$

over these disks is  $\Sigma_g \times D^2$ , restricting to the hyperelliptic quotient in each fiber. A ribbon surface is then constructed by attaching left-handed half-twisted bands so that the core of each band is the arc  $\pi(c_i)$  in  $S^2 \times \{\text{point}\}$ . By the method in [1], in the 2-fold cover of  $S^2 \times D^2$  branched over this ribbon surface, each added band lifts to a 2-handle attached along  $c_i$ , with relative framing  $-1$ . Thus the lift of  $S^2 \times D^2$  branched over the ribbon surface is the total space of a Lefschetz fibration over  $D^2$ , with monodromy factorization  $t_{c_1} \dots t_{c_\mu}$ . On the boundary, we have a  $\Sigma_g$ -bundle over  $S^1$  covering an  $S^2$ -bundle over  $S^1$ , each with monodromy isotopic to the identity. To extend the branched covering over  $W$ , it is necessary to find a *fiber-isotopy* of the factorization  $t_{c_1} \dots t_{c_\mu}$  to the identity (ie an isotopy through homeomorphisms which are all fiber-preserving with respect to  $\pi$ ): using a given fiber-isotopy to the identity, we can then identify the branched covering on the boundary as  $\pi \times \text{id}: \Sigma_g \times S^1 \rightarrow S^2 \times S^1$  and extend the covering as  $\pi \times \text{id}: \Sigma_g \times D^2 \rightarrow S^2 \times D^2$ . The attachment of  $S^2 \times D^2$  to the base matches the boundary of disks  $\{\text{point}\} \times D^2$  to the boundary of the ribbon surface, and in this way we get a closed surface as branch set. The extension attaches a 2-handle union a 4-handle to the diagram of the base, with the 2-handle attached as a meridian to the 0-framed 2-handle. When working with examples, the braid factorization  $h_{\pi(c_1)} \dots h_{\pi(c_\mu)}$  plays a valuable role. The necessary fiber-isotopy to the identity can often be seen by simply observing that the braid factorization is isotopic to the identity by an isotopy that fixes the branch points at all times, in which case one obtains a fiber-isotopy of  $t_{c_1} \dots t_{c_\mu}$  to the identity as its lift. We can also use the braid factorization to compute the framing of the second attached 2-handle and to see how the attaching circle links the boundary of the branch surface. To do this, we select a reference point  $* \in \Sigma_{0,2g+2} \setminus B_{2g+2}^2$ , where  $B_{2g+2}^2$  is a disk containing the branch points, and track a framed neighborhood of  $*$  through the isotopy of  $d_{h(c_1)} \dots d_{h(c_\mu)}$  to the identity.

In [9], it was shown how to modify this branched covering description of a hyperelliptic Lefschetz fibration to accomplish an unchaining monodromy substitution. Although the procedure in [9] was described only for even unchaining substitutions, the method applies equally well to the odd unchaining substitutions considered here.

## 4 The proof of Theorem 1

We are now ready to describe the manifolds  $X'_g(i)$  constructed by Baykur, Hayano, and Monden, and prove that they are diffeomorphic to the elliptic surfaces  $E(g-i)$ .

### 4.1 The manifolds $X'_g(i)$ and $X_g(i)$

In [4], Baykur, Hayano, and Monden construct their infinite family of Lefschetz pencils by explicit monodromy factorization. Their factorizations use Dehn twists about the curves on  $\Sigma_g^{2(i+1)}$  shown in Figure 4. We abbreviate the product of boundary curve twists as  $\Delta = t_{\delta_{i+1}} \dots t_{\delta_2} t_{\delta_1} t_{\delta'_{i+1}} \dots t_{\delta'_2} t_{\delta'_1}$ , and also let  $D_g = t_{d_4} t_{d_5} \dots t_{d_{2g+1}}$  and  $E_g = t_{e_{2g+1}} \dots t_{e_5} t_{e_4}$ .

**Theorem** [4, Theorem 4.6] *For each  $g \geq 3$  and  $0 \leq i \leq g - 1$ , there are symplectic genus  $g$  Lefschetz pencils on  $X'_g(i)$  with monodromy factorizations in  $\Gamma_g^{2(i+1)}$ ,*

$$\Delta = \begin{cases} D_g E_g t_{x_{i+1}} \dots t_{x_2} t_{x_1} t_{x'_{i+1}} \dots t_{x'_2} t_{x'_1} (t_{c_1} t_{c_2} t_{c_3})^{4(g-i)}, & g \text{ odd,} \\ D_g E_g t_{x_{i+1}} \dots t_{x_2} t_{x_1} t_{x'_{i+1}} \dots t_{x'_2} t_{x'_1} (t_{c_1} t_{c_2} t_{c_3})^{4(g-1-i)+2} (t_{c_3} t_{c_2} t_{c_1})^2, & g \text{ even.} \end{cases}$$

(Here we have cyclically permuted the right-hand side from its expression in [4].)

If we cap off each boundary component of  $\Sigma_g^{2(i+1)}$  with a disk, each of the curves  $x_j$  and  $x'_j$  become parallel copies of a curve  $x$  and  $x'$ , respectively, on  $\Sigma_g$ . From the previous equation we see that the monodromy factorization of the Lefschetz fibration  $X_g(i) \rightarrow S^2$  is

$$(2) \quad 1 = \begin{cases} D_g E_g (t_x)^{i+1} (t_{x'})^{i+1} (t_{c_1} t_{c_2} t_{c_3})^{4(g-i)} & \text{if } g \text{ is odd,} \\ D_g E_g (t_x)^{i+1} (t_{x'})^{i+1} (t_{c_1} t_{c_2} t_{c_3})^{4(g-1-i)+2} (t_{c_3} t_{c_2} t_{c_1})^2 & \text{if } g \text{ is even.} \end{cases}$$

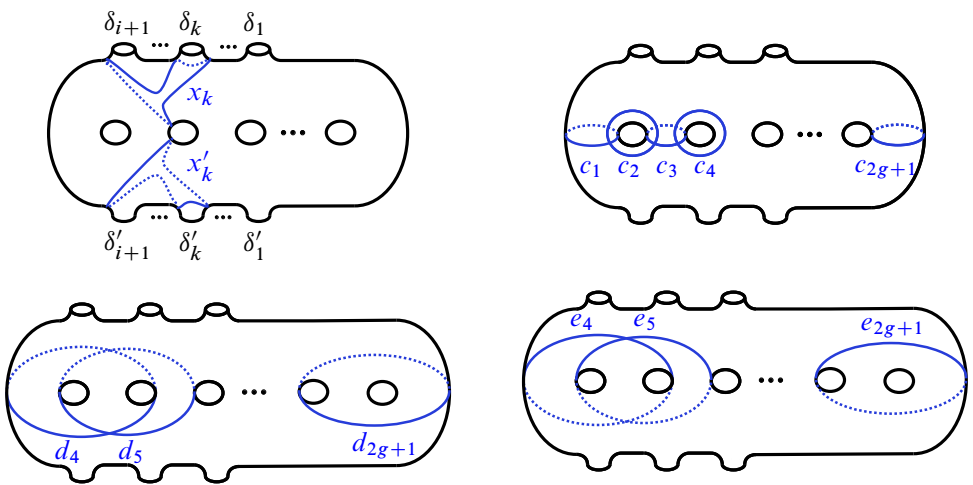


Figure 4: Curves on  $\Sigma_g^{2(i+1)}$ .

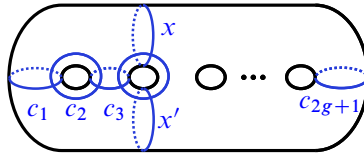


Figure 5: Curves on  $\Sigma_g$ .

As it will play a role later, we review Baykur, Hayano, and Monden’s derivation of this monodromy factorization. They begin with the full chain relation

$$t_{\delta_1} t_{\delta'_1} = (t_{c_1} t_{c_2} \dots t_{c_{2g+1}})^{2g+2}$$

in  $\Gamma_g^2$ . This is well known to be the monodromy of a pencil with two basepoints on a complex surface  $Z'_g$  of general type. Through a series of lemmas, they show this is Hurwitz equivalent to the factorization

$$(3) \quad t_{\delta_1} t_{\delta'_1} = \begin{cases} D_g E_g (t_{c_1} t_{c_2} t_{c_3})^{4g} (t_{c_5} t_{c_6} \dots t_{c_{2g+1}})^{2g-2}, & g \text{ odd,} \\ D_g E_g (t_{c_1} t_{c_2} t_{c_3})^{4(g-1)+2} (t_{c_3} t_{c_2} t_{c_1})^2 (t_{c_5} t_{c_6} \dots t_{c_{2g+1}})^{2g-2}, & g \text{ even.} \end{cases}$$

They then apply unchaining monodromy substitutions to this factorization,  $i$  times to the subword  $(t_{c_1} t_{c_2} t_{c_3})^4$ , and once to  $(t_{c_5} t_{c_6} \dots t_{c_{2g+1}})^{2g-2}$ . In addition, a clever inductive use of the lantern relation shows that this relation has a lift from  $\Gamma_g^2$  to  $\Gamma_g^{2(i+1)}$ , providing enough sections of the pencil to allow for the computation of the symplectic Kodaira dimension for some of the resulting 4–manifolds, and giving the factorization in the above theorem.

We give separate proofs that  $X'_g(i) \cong E(g-i)$  for  $g$  odd and even. Each proof will have two stages: representing  $X'_g(i)$  as a 2–fold branched cover, followed by modifications of the base that realize the diffeomorphism.

## 4.2 The proof for odd $g$

**4.2.1 Representing  $X'_g(i)$  as a branched covering** Let  $\mathbb{F}_n$  denote the  $n^{\text{th}}$  Hirzebruch surface. We begin by discussing how to represent  $X'_g(i)$  for odd  $g$  as the 2–fold branched cover of the rational surface  $\mathbb{F}_{i+1}$ , branched over an embedded surface. The base of the covering and the branch surface will be represented as a banded unlink diagram.

Recalling the derivation of the factorization in the theorem of Section 4.1, we discuss first the Lefschetz fibration  $Z_g \rightarrow S^2$  that comes from blowing up the Lefschetz pencil defined by (3). This Lefschetz fibration on  $Z_g$  has monodromy given by the relation

$$(4) \quad D_g E_g (t_{c_1} t_{c_2} t_{c_3})^{4i} (t_{c_5} t_{c_6} \dots t_{c_{2g+1}})^{2g-2} (t_{c_1} t_{c_2} t_{c_3})^{4(g-i)} = 1$$

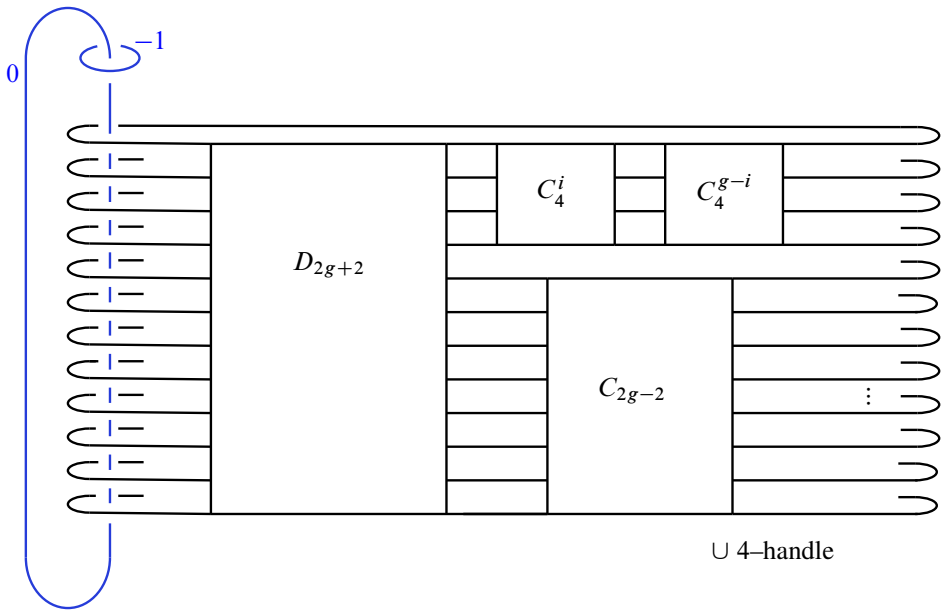


Figure 6: The 2-fold branched cover is  $Z_g$ .

in  $\Gamma_g$ . This is a hyperelliptic Lefschetz fibration, and from the discussion in Section 3, we see that  $Z_g$  can be described as the 2-fold cover of  $\mathbb{F}_1$  branched over the surface described in Figure 6. The visible part of the branch surface is the ribbon surface consisting of  $2g + 2$  horizontal disks together with the collection of bands  $C_4$ ,  $C_{2g-2}$ , and  $D_{2g+2}$  defined in Figures 7 and 8. (The exponents for  $C_4$  denote repeated copies.) The branched cover of the 0-handle union the 0-framed 2-handle branched over the ribbon surface is a Lefschetz fibration over  $D^2$  with monodromy given by (4). It can be checked directly using the Alexander method (see [7]) that the projection of (4)

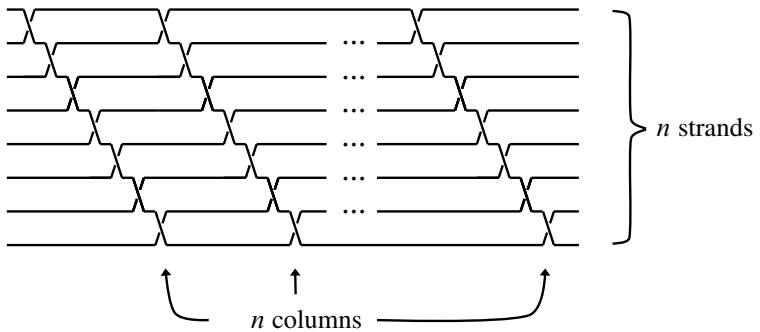


Figure 7: The braid  $C_n$ .

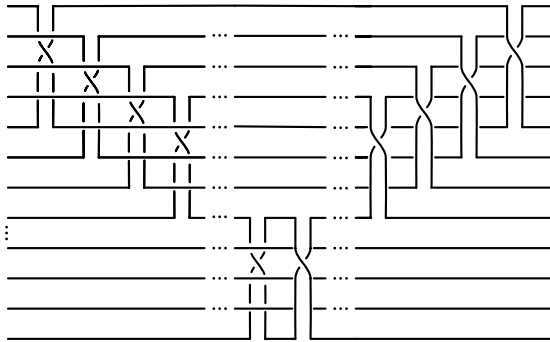


Figure 8: The braid  $D_n$ , with  $n$  strands.

to a homeomorphism of  $\Sigma_{0,2g+2}$  equals a right-handed Dehn twist about a circle which encloses all marked branch points. This is isotopic to the identity by an isotopy that fixes all branch points throughout, providing a fiber-isotopy to the identity, as required. This isotopy also fixes a reference point  $*$   $\in \Sigma_{0,2g+2} \setminus B_{2g+2}^2$ , and rotates a framed neighborhood of  $*$  once in a left-handed direction. Thus if we attach the second 2–handle as shown in Figure 6, along a meridian with framing  $-1$ , we match  $2g + 2$  disks to the boundary of the ribbon surface, and we see  $Z_g$  as the cover of the surface given as a banded unlink diagram, as claimed.

We now consider unchaining substitutions on (4),  $i$  times on the subword  $(t_{c_1}t_{c_2}t_{c_3})^{4i}$  and once on  $(t_{c_5}t_{c_6} \dots t_{c_{2g+1}})^{2g-2}$ . Doing so yields Baykur, Hayano, and Monden’s relation (2) that defines the Lefschetz fibration  $X_g(i)$ . As described in [9], we can realize this substitution pictorially by “blowing up” the chain boxes in Figure 6, that is, by replacing them with  $-1$ –framed 2–handles, as shown in Figure 9. Each of the newly introduced 2–handles will lift to two 2–handles with relative product framing  $-1$ , attached along the pair of vanishing cycles  $x$  and  $x'$ . This figure still represents a banded unlink diagram, with  $2g + 2$  disks in the 4–handle, attached to the boundary of the ribbon surface. Thus  $X_g(i)$  is the 2–fold cover of  $\mathbb{F}_1 \# (i + 1)\overline{\mathbb{C}\mathbb{P}^2}$  branched over the surface shown in Figure 9.

We next execute a series of moves to the base of the branched covering. We begin by isotoping the newly added 2–handles by swinging them around the back of the ribbon surface so that they appear on the left, as in Figure 10.

We next slide the upper left  $-1$ –framed 2–handle over the lower one, producing Figure 11. Next the  $-2$ –framed 2–handle is slid over the parallel  $0$ –framed one, giving

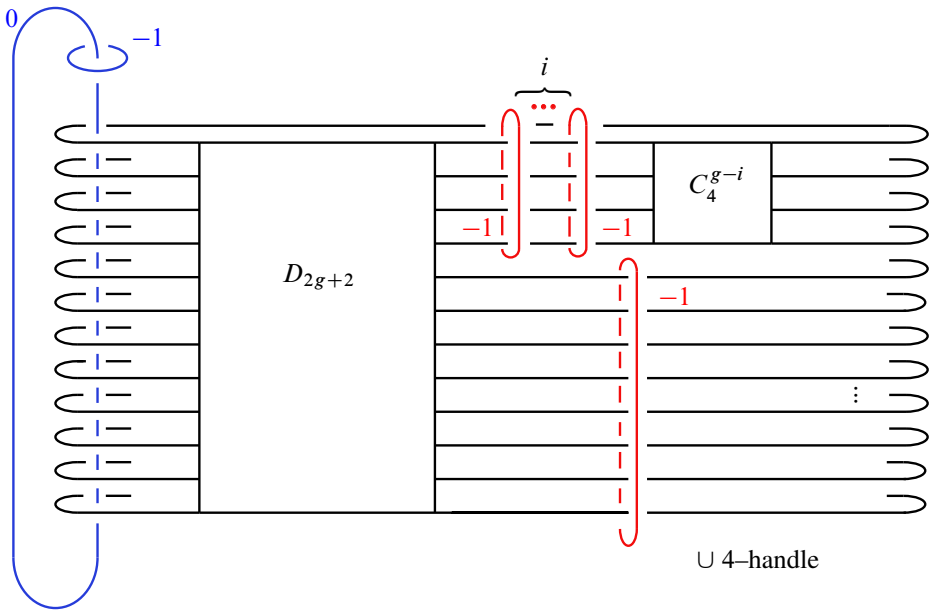


Figure 9: The 2-fold branched cover is  $X_g(i)$ .

Figure 12, and then slid over the  $-1$ -framed 2-handle that links it as a meridian. The result is Figure 13.

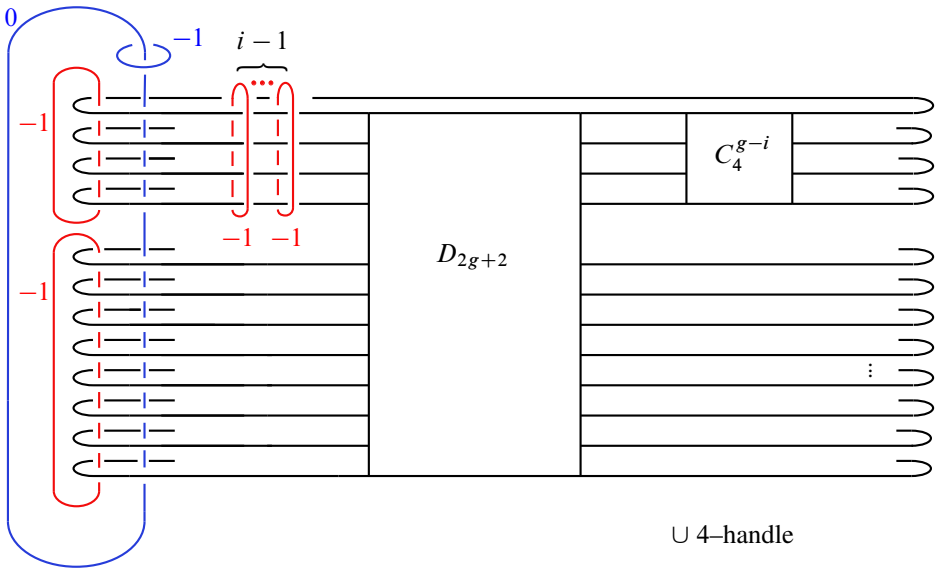


Figure 10



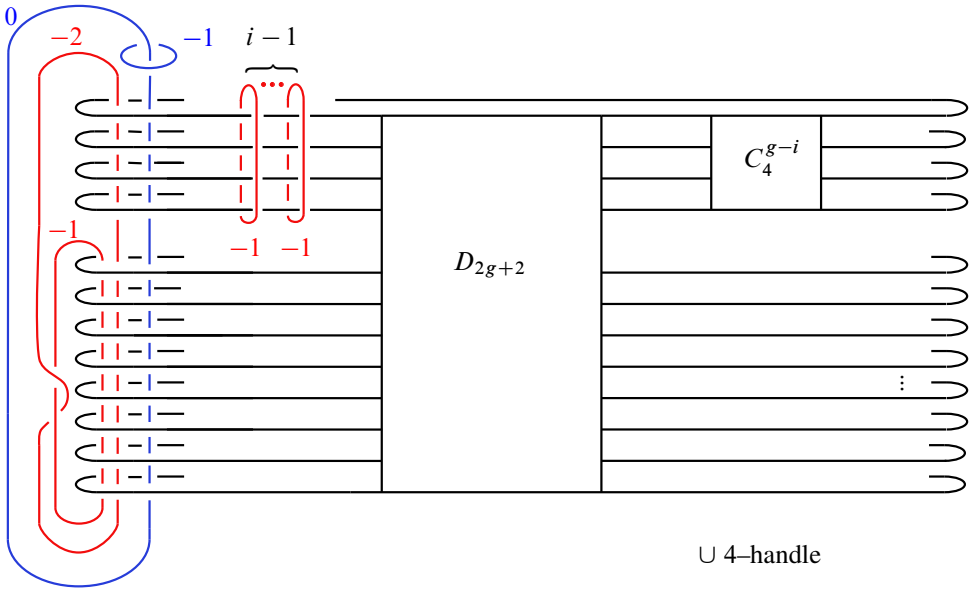


Figure 11

We repeat this series of slides for each of the remaining  $-1$ -framed  $2$ -handles at the top of the picture, resulting in Figure 14.

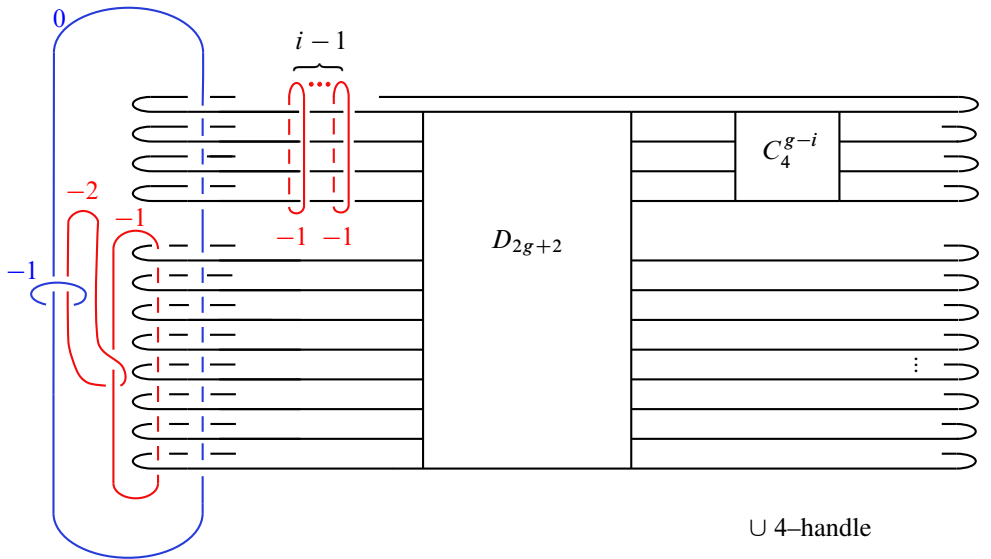


Figure 12

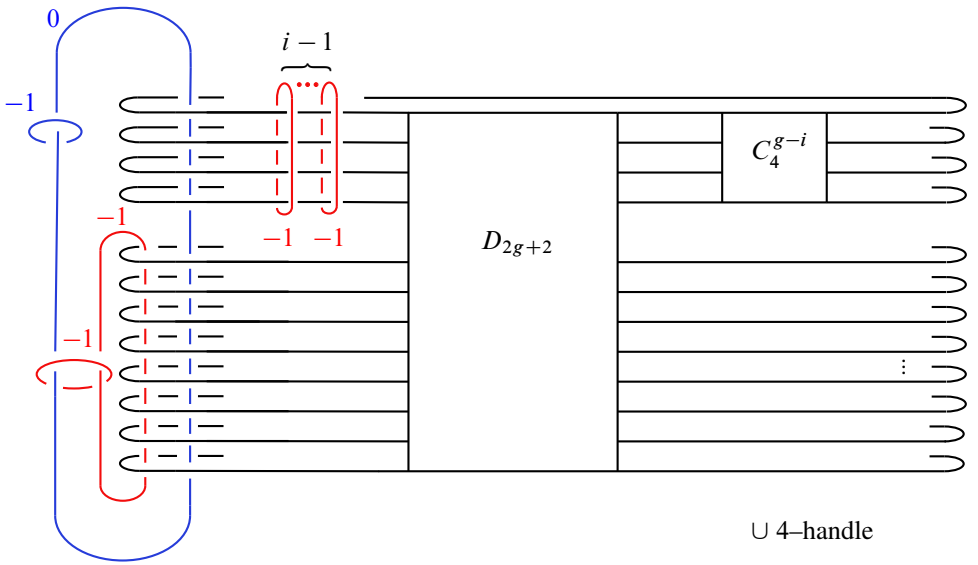


Figure 13

Next we slide the lower  $-1$ -framed  $2$ -handle over the blue  $0$ -framed  $2$ -handle, then slide the result over the (blue)  $-1$ -framed  $2$ -handle, giving Figure 15. Finally, we blow

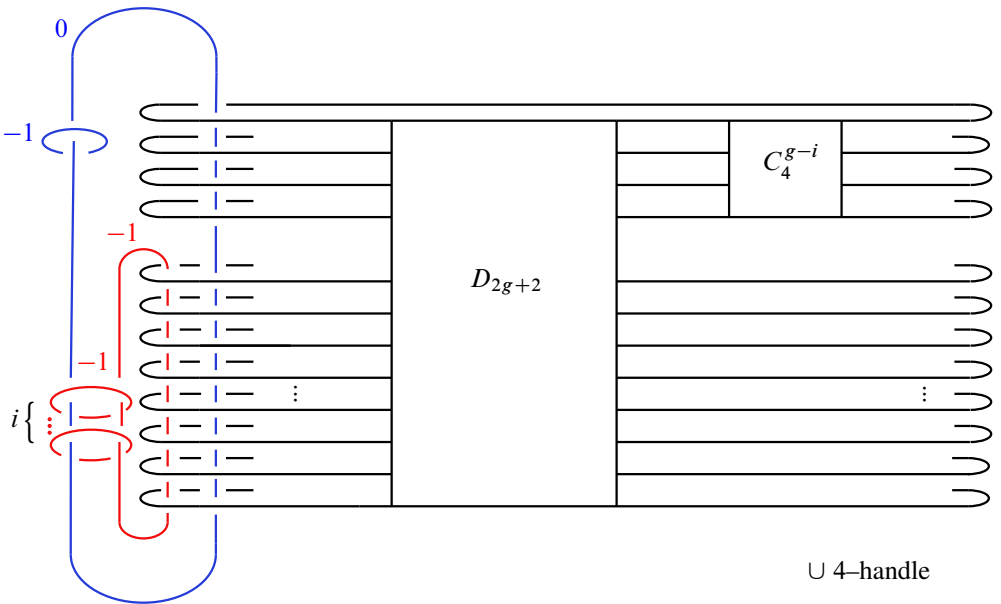


Figure 14

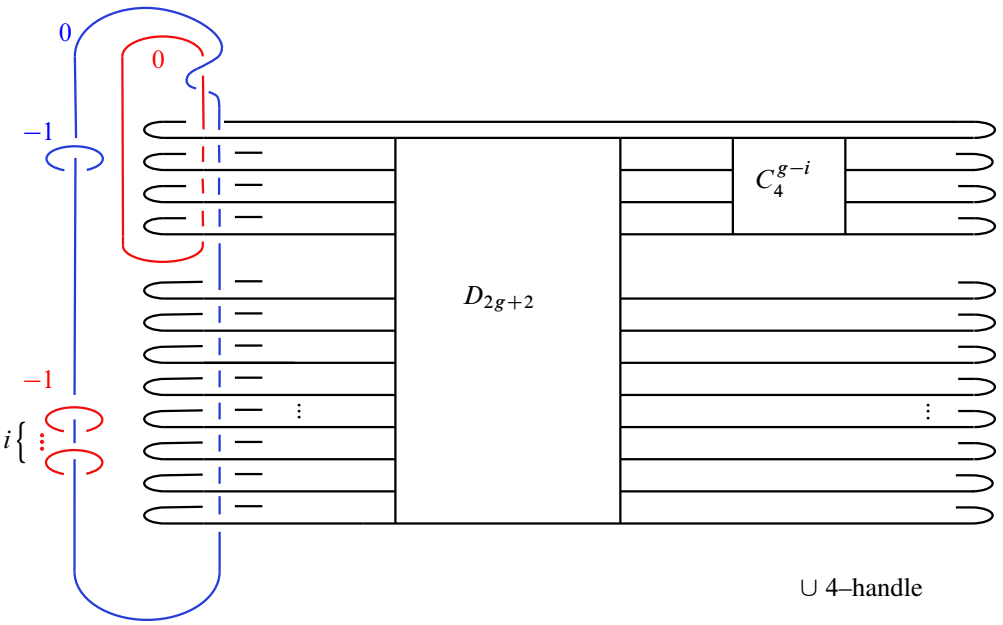


Figure 15

down each of the  $-1$ -framed  $2$ -handles that link the  $0$ -framed  $2$ -handle, to arrive at Figure 16.

We pause here for an important observation: in this last step, each of the  $2$ -handles that we are blowing down are attached along meridians to the  $0$ -framed  $2$ -handle.

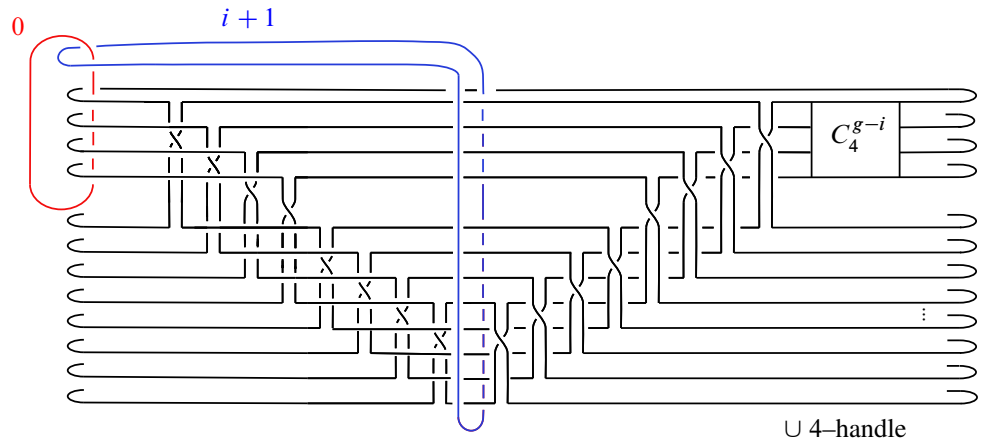


Figure 16: The  $2$ -fold branched cover is  $X'_g(i)$ .

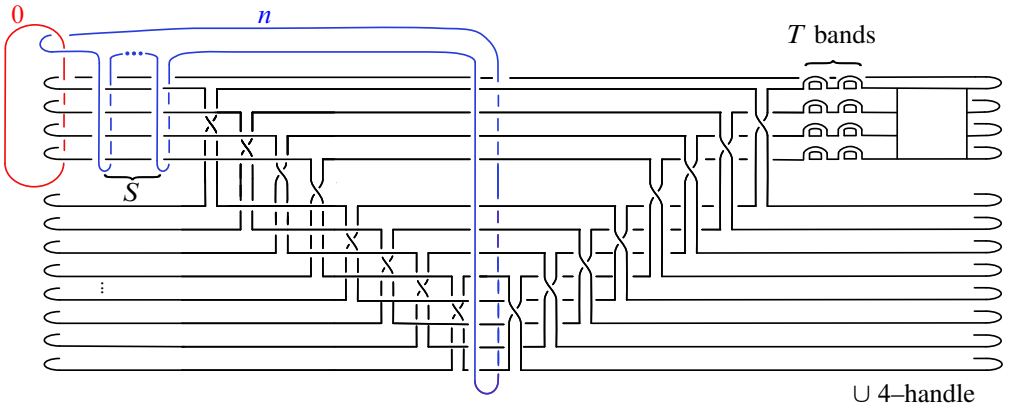


Figure 17: The ribbon surface  $F(R, S, T)$  has  $R$  horizontal disks.

Retracing the diffeomorphism that goes between Figures 16 and 9, we see that the spheres given by these handles will each lift to two sections of the Lefschetz fibration on  $X_g(i)$ , of square  $-1$ . Because we have blown down  $2(i + 1)$  sections of the fibration  $X_g(i)$  with square  $-1$ , it follows that the 2-fold branched cover of  $\mathbb{F}_{i+1}$  branched over the embedded surface described in Figure 16 is  $X'_g(i)$ .

We next show that description of  $X'_g(i)$  as the branched cover in Figure 16 can be used to show that it is diffeomorphic to  $E(g - i)$ . This relies on a key lemma.

**4.2.2 A key lemma** To set up the statement, let  $F(R, S, T)$  denote any ribbon surface in the 4-manifold  $\mathbb{F}_n$  of the form shown in Figure 17. The box can represent

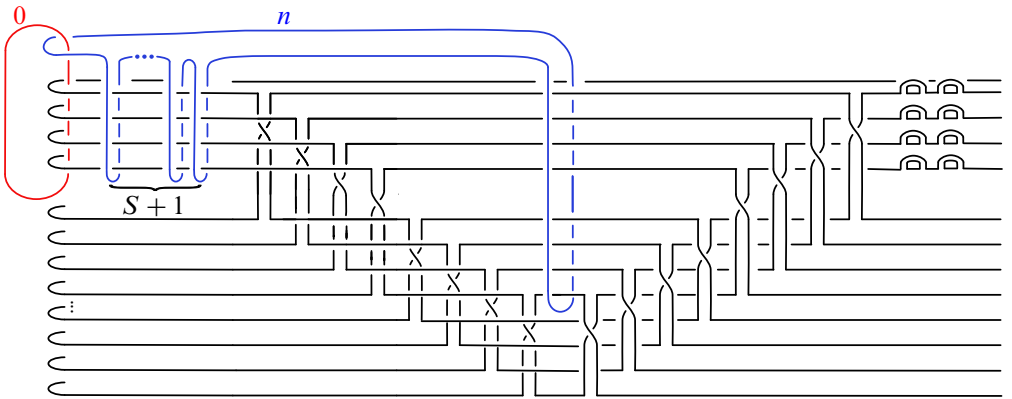


Figure 18

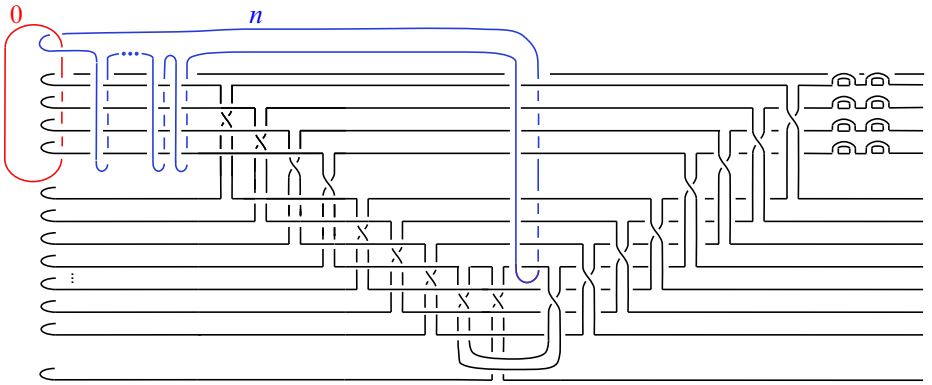


Figure 19

any collection of bands, with the condition that any bands located there are attached to the top four horizontal disks, and avoid the disks below.

The notation records that

- the ribbon surface has  $R$  horizontal disks,
- the  $n$ -framed attaching circle links the horizontal disks  $S$  times positively in the indicated region, and
- there are  $T$  trivial bands attached to the top four horizontal disks.

In applications of Lemma 7,  $T$  will be divisible by four, and the trivial bands will be distributed evenly among the top four horizontal disks.

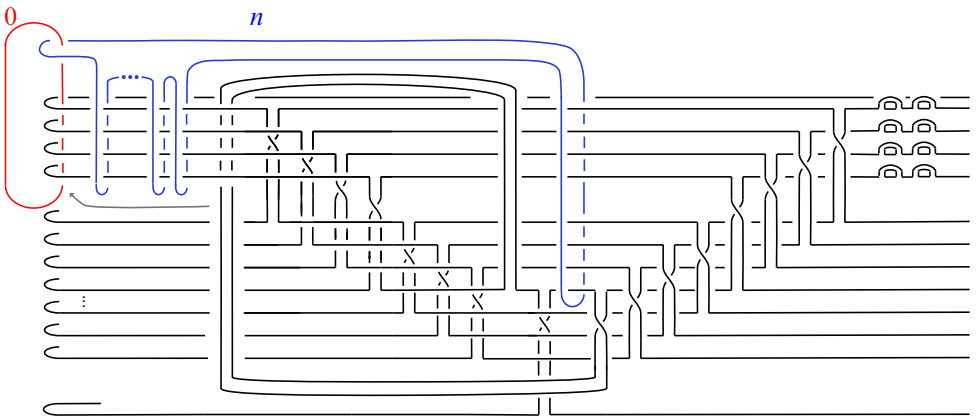


Figure 20

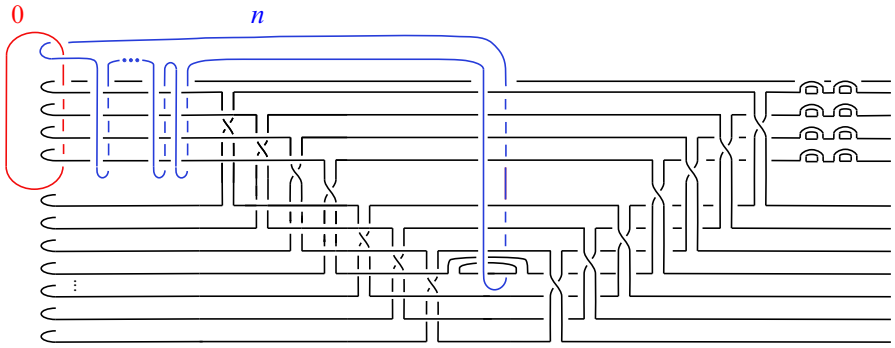


Figure 21

**Lemma 7** For  $R \geq 8$ , the ribbon surface  $F(R, S, T)$  is isotopic to the ribbon surface  $F(R - 4, S + 1, T + 4)$ .

**Proof** Beginning with  $F(R, S, T)$  as shown in Figure 17, we obtain Figure 18 by a 2–handle band dive of the  $n$ –framed 2–handle. This increases the linking in the upper left of the picture to  $S + 1$ . A band slide results in Figure 19, and a band dive of that same band gives Figure 20.

At this point, we may cancel the bottom horizontal disk with the remaining attached band. In addition, we do a 2–handle band slide over the 0–framed 2–handle, using a band indicated by the gray arrow; the slide disengages the band from the top four horizontal disks, and it can be isotoped to the trivial band shown in Figure 21.

The transition from Figure 18 to Figure 21 resulted in the cancellation of the bottom horizontal disk, and added a trivial band in the process. We can repeat these steps three

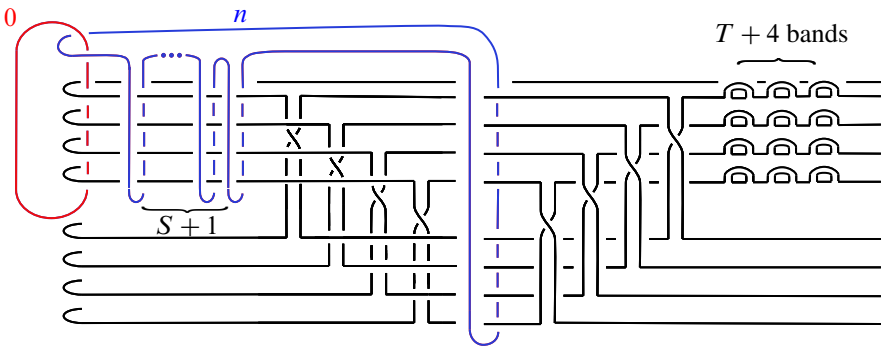


Figure 22

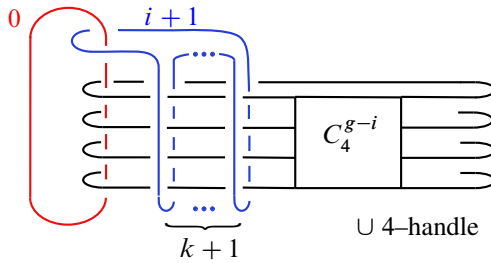


Figure 23

times to remove the bottom three horizontal disks, as shown in Figure 22. In this figure, we have moved the trivial bands from their position in Figure 21, by sliding them over the long bands to their right, so that they are now attached to the top four disks. In total we have removed the four bottom horizontal disks, and added four trivial bands; thus the values of  $R$  and  $T$  change to  $R - 4$  and  $T + 4$ , respectively.  $\square$

**4.2.3 An isotopy of the branch surface** Let  $g = 2k + 1$ . Returning to the proof of Theorem 1, Figure 16 shows that  $X'_g(i)$  is diffeomorphic to the 2-fold branched cover of  $\mathbb{F}_{i+1}$  branched over a surface of the form  $F(2g + 2, 0, 0) = F(4k + 4, 0, 0)$ . Then  $k$  iterations of Lemma 7 give that  $X'_g(i)$  is diffeomorphic to the 2-fold branched cover branched over a surface of the form  $F(4, k, 4k)$ . Recall that the full surface in Figure 16 includes  $2g + 2$  unseen disks attached to the boundary of the ribbon surface, with their interiors in the 4-handle. Using  $4k = 2g - 2$  of these disks to cancel the trivial bands, we have that  $X'_g(i)$  is diffeomorphic to the cover of the manifold in Figure 23. (Note that four disks remain in the 4-handle.) We arrive at Figure 24 by sliding the  $(i + 1)$ -framed 2-handle over the 0-framed one  $k + 1$  times. The new framing is  $(i + 1) - 2(k + 1) = i - 2k - 1 = -(g - i)$ , as shown.

The proof for odd  $g$  is completed by recognizing that the branched cover of  $\mathbb{F}_{g-i}$  over the surface in Figure 24 is  $E(g - i)$ . This is immediate from the discussion

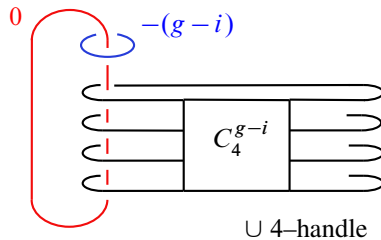


Figure 24

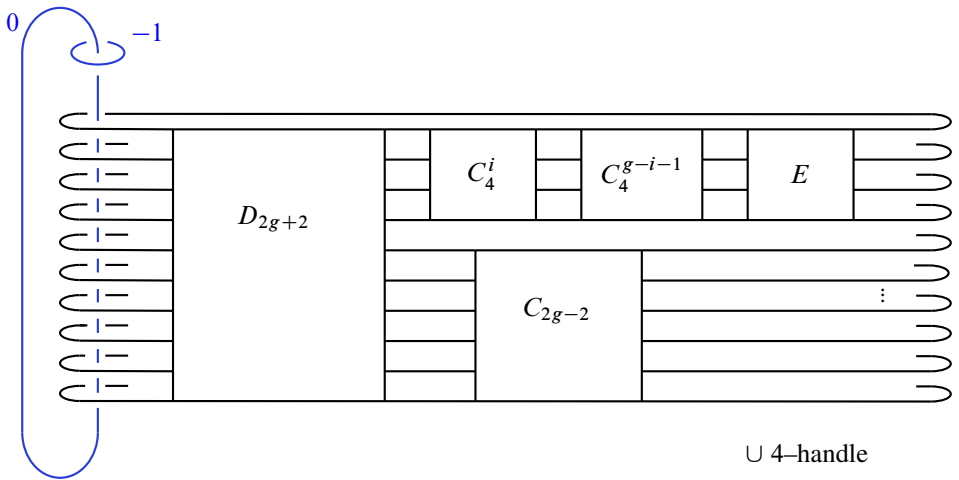


Figure 25

in Section 3. The lift of the branched cover of the 0–handle union the 0–framed 2–handle branched over the ribbon surface is a genus 1 Lefschetz fibration over  $D^2$  with monodromy  $(t_{c_1}t_{c_2}t_{c_3})^{4(g-i)}$ . The braid  $(d_{\pi(c_1)}d_{\pi(c_2)}d_{\pi(c_3)})^{4(g-i)}$  is equal to  $g - i$  full right-handed Dehn twists about a circle enclosing all branch points. This isotopy of this to the identity fixes a reference point in  $\Sigma_{0,4} \setminus B_4^2$  while rotating a framed neighborhood  $g - i$  times in a left-handed direction. Thus adding a 2–handle with the indicated location and framing shows that the branched cover of  $\mathbb{F}_{g-i}$  over the rest of the surface extends to a total space which is a genus 1 Lefschetz fibration over  $S^2$ , whose monodromy matches a well-known factorization of  $E(g - i)$ .

### 4.3 The proof for even $g$

The proof for even  $g$  is essentially the same as for odd  $g$ . However, because  $2g + 2$  is no longer divisible by four, we must include two additional iterations of the basic moves used in the proof of Lemma 7. Also, because the different form of the monodromy of  $X'_g(i)$  makes for a different ribbon branch surface, the final step of recognizing the total space of the cover as an elliptic surface is somewhat different.

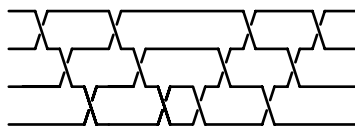


Figure 26: The ribbon surface  $E$ .



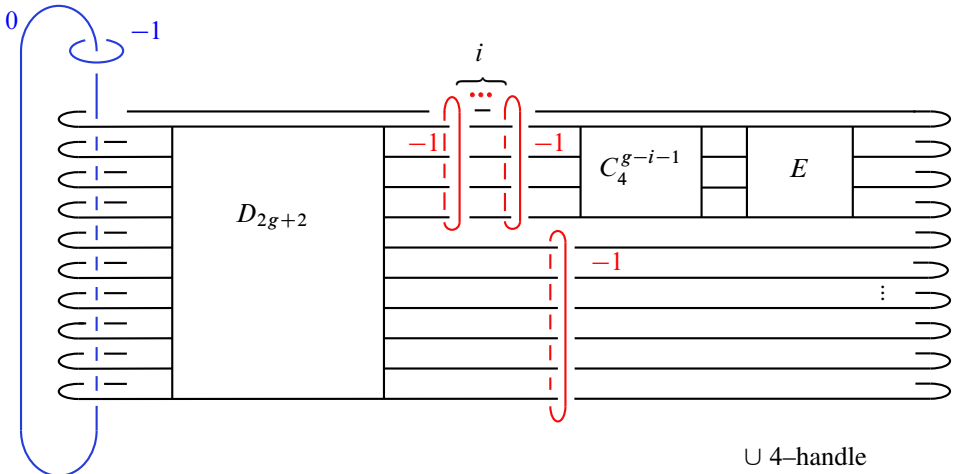


Figure 27

As a starting point for even  $g$ , we begin with the Lefschetz fibration on  $Z_g$ , which from (3) has a monodromy factorization given by the relation

$$(5) \quad D_g E_g (t_{c_1} t_{c_2} t_{c_3})^{4i} (t_{c_5} t_{c_6} \dots t_{c_{2g+1}})^{2g-2} (t_{c_1} t_{c_2} t_{c_3})^{4(g-i-1)} (t_{c_1} t_{c_2} t_{c_3})^2 (t_{c_3} t_{c_2} t_{c_1})^2 = 1.$$

As before, this hyperelliptic Lefschetz fibration can be described as the 2-fold cover of  $\mathbb{F}_1$  branched over the surface described in Figures 25 and 26. Once again, it can be checked that the projection of (5) to a homeomorphism of  $\Sigma_{0,2g+2}$  equals a right-handed Dehn twist about a circle that encloses all marked branch points. The unseen part of the branch surface is  $2g + 2$  disks attached to the boundary of the ribbon surface,

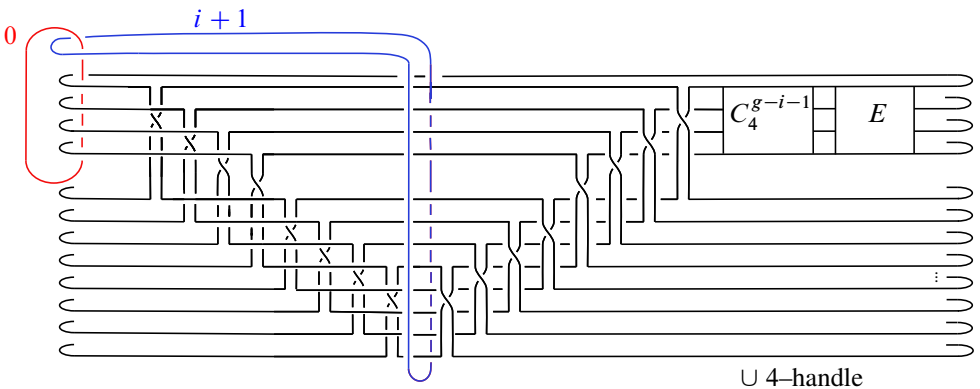


Figure 28

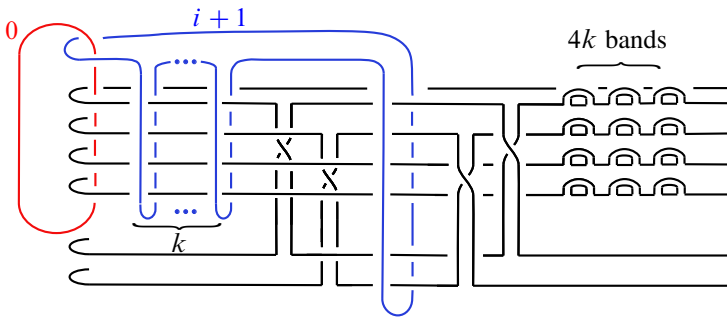


Figure 29

with interiors in the 4–handle, exactly as in the odd  $g$  case. Thus Figure 25 depicts a banded unlink diagram, as before.

Performing unchaining monodromy substitutions gives that  $X_g(i)$  is the 2–fold cover of  $\mathbb{F}_1 \# (i + 1)\mathbb{C}\mathbb{P}^2$ , branched over the surface in Figure 27. Mimicking the 2–handle slides from the odd case yields  $2(i + 1)$  sections which are blown down to give  $X'_g(i)$  as the 2–fold cover of  $\mathbb{F}_{i+1}$  branched over the surface in Figure 28.

Let  $g = 2k + 2$ . The ribbon surface in Figure 28 is of the form

$$F(2g + 2, 0, 0) = F(4k + 6, 0, 0).$$

Then  $k$  iterations of Lemma 7 give that  $X'_g(i)$  is diffeomorphic to the cover of  $\mathbb{F}_{i+1}$  branched over  $F(6, k, 4k)$ , shown in Figure 29.

We next cancel the bottom two horizontal disks as follows. A 2–handle band dive gives Figure 30. We can then twice more use the sequence of moves in the proof of Lemma 7: a band slide, followed by a band dive, followed by a 2–handle band slide. (See the transition from Figure 18 to Figure 21.) This adds two more trivial bands to

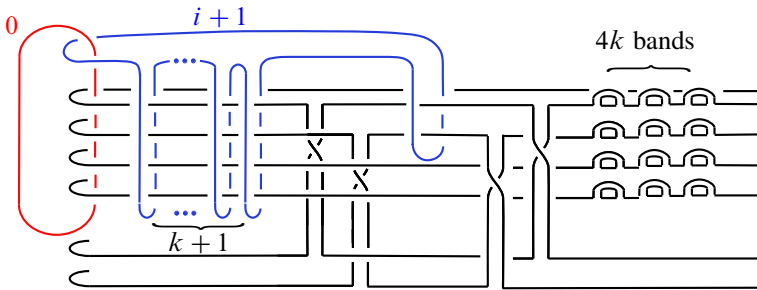


Figure 30

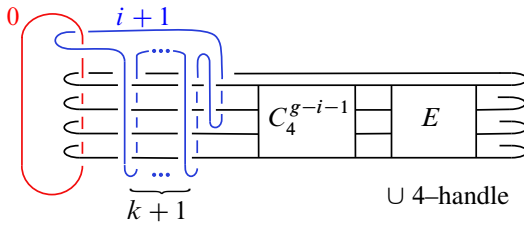


Figure 31

the picture, but we cancel all  $4k + 2 = 2g - 2$  of them using disks from the 4–handle. This results in Figure 31.

We next slide the  $(i + 1)$ –framed 2–handle  $k + 1$  times over the 0–framed handle. The new framing is  $(i + 1) - 2(k + 1) = i - 2k - 1 = -(g - i - 1)$ . This is Figure 32.

It remains to see that the branched cover described by Figure 32, right, is  $E(g - i)$ . The lift of the branched cover of the 0–handle union the 0–framed 2–handle branched over the ribbon surface is a genus 1 Lefschetz fibration over  $D^2$  with monodromy

$$(t_{c_1} t_{c_2} t_{c_3})^{4(g-i-1)} (t_{c_1} t_{c_2} t_{c_3})^2 (t_{c_3} t_{c_2} t_{c_1})^2.$$

The location and framing of the other attaching circle is explained by tracking a framed neighborhood of a reference point  $* \in \Sigma_{0,2g+2} \setminus B_{2g+2}^2$  through an isotopy from the braid

$$(d_{\pi(c_1)} d_{\pi(c_2)} d_{\pi(c_3)})^{4(g-i-1)} (d_{\pi(c_1)} d_{\pi(c_2)} d_{\pi(c_3)})^2 (d_{\pi(c_3)} d_{\pi(c_2)} d_{\pi(c_1)})^2$$

to the identity. This isotopy first undoes  $g - i - 1$  right-handed Dehn twists, which fixes  $*$  while rotating its neighborhood  $g - i - 1$  times oppositely, followed by an isotopy that pushes  $*$  around a circle passing through the middle two marked points without twisting its neighborhood. Thus the branched cover of  $\mathbb{F}_{g-i-1}$  extended over the rest of the surface gives a total space which is a genus 1 Lefschetz fibration over  $S^2$ . Finally, we note that the monodromy factorization of this fibration is easily seen to be equivalent to other well-known factorizations for elliptic fibrations on  $E(g - i)$ .

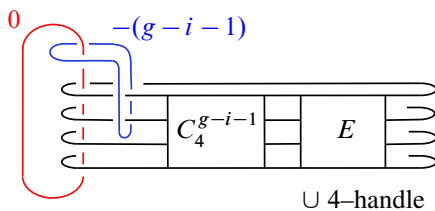


Figure 32

## References

- [1] **S Akbulut, R Kirby**, *Branched covers of surfaces in 4-manifolds*, Math. Ann. 252 (1979/80) 111–131 [MR](#) [Zbl](#)
- [2] **S Bauer**, *Almost complex 4-manifolds with vanishing first Chern class*, J. Differential Geom. 79 (2008) 25–32 [MR](#) [Zbl](#)
- [3] **R I Baykur, K Hayano**, *Multisections of Lefschetz fibrations and topology of symplectic 4-manifolds*, Geom. Topol. 20 (2016) 2335–2395 [MR](#) [Zbl](#)
- [4] **R I Baykur, K Hayano, N Monden**, *Unchaining surgery and topology of symplectic 4-manifolds*, Math. Z. 303 (2023) art. id. 77 [MR](#) [Zbl](#)
- [5] **J S Birman, H M Hilden**, *On isotopies of homeomorphisms of Riemann surfaces*, Ann. of Math. 97 (1973) 424–439 [MR](#) [Zbl](#)
- [6] **S K Donaldson**, *Lefschetz pencils on symplectic manifolds*, J. Differential Geom. 53 (1999) 205–236 [MR](#) [Zbl](#)
- [7] **B Farb, D Margalit**, *A primer on mapping class groups*, Princeton Mathematical Series 49, Princeton Univ. Press (2012) [MR](#) [Zbl](#)
- [8] **S Friedl, S Vidussi**, *On the topology of symplectic Calabi–Yau 4-manifolds*, J. Topol. 6 (2013) 945–954 [MR](#) [Zbl](#)
- [9] **T Fuller**, *Hyperelliptic Lefschetz fibrations and branched covering spaces*, Pacific J. Math. 196 (2000) 369–393 [MR](#) [Zbl](#)
- [10] **R E Gompf, A I Stipsicz**, *4-Manifolds and Kirby calculus*, Graduate Studies in Math. 20, Amer. Math. Soc., Providence, RI (1999) [MR](#) [Zbl](#)
- [11] **M C Hughes, S Kim, M Miller**, *Isotopies of surfaces in 4-manifolds via banded unlink diagrams*, Geom. Topol. 24 (2020) 1519–1569 [MR](#) [Zbl](#)
- [12] **A Kas**, *On the handlebody decomposition associated to a Lefschetz fibration*, Pacific J. Math. 89 (1980) 89–104 [MR](#) [Zbl](#)
- [13] **T-J Li**, *Quaternionic bundles and Betti numbers of symplectic 4-manifolds with Kodaira dimension zero*, Int. Math. Res. Not. 2006 (2006) art. id. 37385 [MR](#) [Zbl](#)
- [14] **T-J Li**, *Symplectic 4-manifolds with Kodaira dimension zero*, J. Differential Geom. 74 (2006) 321–352 [MR](#) [Zbl](#)
- [15] **I Smith**, *Lefschetz pencils and divisors in moduli space*, Geom. Topol. 5 (2001) 579–608 [MR](#) [Zbl](#)

Department of Mathematics, California State University, Northridge  
Northridge, CA, United States

[terry.fuller@csun.edu](mailto:terry.fuller@csun.edu)

Received: 23 August 2021      Revised: 30 November 2021

# ALGEBRAIC & GEOMETRIC TOPOLOGY

[msp.org/agt](http://msp.org/agt)

## EDITORS

### PRINCIPAL ACADEMIC EDITORS

John Etnyre  
[etnyre@math.gatech.edu](mailto:etnyre@math.gatech.edu)  
Georgia Institute of Technology

Kathryn Hess  
[kathryn.hess@epfl.ch](mailto:kathryn.hess@epfl.ch)  
École Polytechnique Fédérale de Lausanne

### BOARD OF EDITORS

Julie Bergner	University of Virginia <a href="mailto:jeb2md@eservices.virginia.edu">jeb2md@eservices.virginia.edu</a>	Robert Lipshitz	University of Oregon <a href="mailto:lipshitz@uoregon.edu">lipshitz@uoregon.edu</a>
Steven Boyer	Université du Québec à Montréal <a href="mailto:cohf@math.rochester.edu">cohf@math.rochester.edu</a>	Norihiko Minami	Nagoya Institute of Technology <a href="mailto:nori@nitech.ac.jp">nori@nitech.ac.jp</a>
Tara E. Brendle	University of Glasgow <a href="mailto:tara.brendle@glasgow.ac.uk">tara.brendle@glasgow.ac.uk</a>	Andrés Navas	Universidad de Santiago de Chile <a href="mailto:andres.navas@usach.cl">andres.navas@usach.cl</a>
Indira Chatterji	CNRS & Université Côte d'Azur (Nice) <a href="mailto:indira.chatterji@math.cnrs.fr">indira.chatterji@math.cnrs.fr</a>	Thomas Nikolaus	University of Münster <a href="mailto:nikolaus@uni-muenster.de">nikolaus@uni-muenster.de</a>
Alexander Dranishnikov	University of Florida <a href="mailto:dranish@math.ufl.edu">dranish@math.ufl.edu</a>	Robert Oliver	Université Paris 13 <a href="mailto:bobol@math.univ-paris13.fr">bobol@math.univ-paris13.fr</a>
Corneli Druţu	University of Oxford <a href="mailto:cornelia.drutu@maths.ox.ac.uk">cornelia.drutu@maths.ox.ac.uk</a>	Birgit Richter	Universität Hamburg <a href="mailto:birgit.richter@uni-hamburg.de">birgit.richter@uni-hamburg.de</a>
Tobias Ekholm	Uppsala University, Sweden <a href="mailto:tobias.ekholm@math.uu.se">tobias.ekholm@math.uu.se</a>	Jérôme Scherer	École Polytech. Féd. de Lausanne <a href="mailto:jerome.scherer@epfl.ch">jerome.scherer@epfl.ch</a>
Mario Eudave-Muñoz	Univ. Nacional Autónoma de México <a href="mailto:mario@matem.unam.mx">mario@matem.unam.mx</a>	Zoltán Szabó	Princeton University <a href="mailto:szabo@math.princeton.edu">szabo@math.princeton.edu</a>
David Futер	Temple University <a href="mailto:dfuter@temple.edu">dfuter@temple.edu</a>	Ulrike Tillmann	Oxford University <a href="mailto:tillmann@maths.ox.ac.uk">tillmann@maths.ox.ac.uk</a>
John Greenlees	University of Warwick <a href="mailto:john.greenlees@warwick.ac.uk">john.greenlees@warwick.ac.uk</a>	Maggy Tomova	University of Iowa <a href="mailto:maggy-tomova@uiowa.edu">maggy-tomova@uiowa.edu</a>
Ian Hambleton	McMaster University <a href="mailto:ian@math.mcmaster.ca">ian@math.mcmaster.ca</a>	Nathalie Wahl	University of Copenhagen <a href="mailto:wahl@math.ku.dk">wahl@math.ku.dk</a>
Hans-Werner Henn	Université Louis Pasteur <a href="mailto:henn@math.u-strasbg.fr">henn@math.u-strasbg.fr</a>	Chris Wendl	Humboldt-Universität zu Berlin <a href="mailto:wendl@math.hu-berlin.de">wendl@math.hu-berlin.de</a>
Daniel Isaksen	Wayne State University <a href="mailto:isaksen@math.wayne.edu">isaksen@math.wayne.edu</a>	Daniel T. Wise	McGill University, Canada <a href="mailto:daniel.wise@mcgill.ca">daniel.wise@mcgill.ca</a>
Christine Lescop	Université Joseph Fourier <a href="mailto:lescop@ujf-grenoble.fr">lescop@ujf-grenoble.fr</a>		

---

See inside back cover or [msp.org/agt](http://msp.org/agt) for submission instructions.


The subscription price for 2023 is US \$650/year for the electronic version, and \$940/year (+ \$70, if shipping outside the US) for print and electronic. Subscriptions, requests for back issues and changes of subscriber address should be sent to MSP. Algebraic & Geometric Topology is indexed by [Mathematical Reviews](#), [Zentralblatt MATH](#), [Current Mathematical Publications](#) and the [Science Citation Index](#).

Algebraic & Geometric Topology (ISSN 1472-2747 printed, 1472-2739 electronic) is published 9 times per year and continuously online, by Mathematical Sciences Publishers, c/o Department of Mathematics, University of California, 798 Evans Hall #3840, Berkeley, CA 94720-3840. Periodical rate postage paid at Oakland, CA 94615-9651, and additional mailing offices. POSTMASTER: send address changes to Mathematical Sciences Publishers, c/o Department of Mathematics, University of California, 798 Evans Hall #3840, Berkeley, CA 94720-3840.

---

AGT peer review and production are managed by EditFlow<sup>®</sup> from MSP.

PUBLISHED BY

 **mathematical sciences publishers**  
nonprofit scientific publishing

<http://msp.org/>

© 2023 Mathematical Sciences Publishers

# ALGEBRAIC & GEOMETRIC TOPOLOGY

Volume 23

Issue 6 (pages 2415–2924)

2023

---

An algorithmic definition of Gabai width	2415
RICKY LEE	
Classification of torus bundles that bound rational homology circles	2449
JONATHAN SIMONE	
A mnemonic for the Lipshitz–Ozsváth–Thurston correspondence	2519
ARTEM KOTELSKIY, LIAM WATSON and CLAUDIUS ZIBROWIUS	
New bounds on maximal linkless graphs	2545
RAMIN NAIMI, ANDREI PAVELESCU and ELENA PAVELESCU	
Legendrian large cables and new phenomenon for nonuniformly thick knots	2561
ANDREW MCCULLOUGH	
Homology of configuration spaces of hard squares in a rectangle	2593
HANNAH ALPERT, ULRICH BAUER, MATTHEW KAHLE, ROBERT MACPHERSON and KELLY SPENDLOVE	
Nonorientable link cobordisms and torsion order in Floer homologies	2627
SHERRY GONG and MARCO MARENGON	
A uniqueness theorem for transitive Anosov flows obtained by gluing hyperbolic plugs	2673
FRANÇOIS BÉGUIN and BIN YU	
Ribbon 2–knot groups of Coxeter type	2715
JENS HARLANDER and STEPHAN ROSEBROCK	
Weave-realizability for $D$ –type	2735
JAMES HUGHES	
Mapping class groups of surfaces with noncompact boundary components	2777
RYAN DICKMANN	
Pseudo-Anosov homeomorphisms of punctured nonorientable surfaces with small stretch factor	2823
SAYANTAN KHAN, CALEB PARTIN and REBECCA R WINARSKI	
Infinitely many arithmetic alternating links	2857
MARK D BAKER and ALAN W REID	
Unchaining surgery, branched covers, and pencils on elliptic surfaces	2867
TERRY FULLER	
Bifiltrations and persistence paths for 2–Morse functions	2895
RYAN BUDNEY and TOMASZ KACZYNSKI	